Science Robotics
AAAS

Supplementary Materials for

Liquid-amplified zipping actuators for micro-air vehicles with transmission-free flapping

Tim Helps *et al.*

Corresponding author: Jonathan Rossiter, jonathan.rossiter@bristol.ac.uk

Sci. Robot. **7**, eabi8189 (2022)
DOI: 10.1126/scirobotics.abi8189

This PDF file includes:

Materials and Methods

Wing electrode modelling. Fig. S5 shows a diagram of a wing electrode of length L in bending, along with a section of the electrode of length dx at a distance from the wing root x. $w(x,t)$ is the displacement of the electrode from its rest position, which varies with position along the electrode x and time t. M and V are the moment and shear force acting on the electrode section at that position, respectively. Taking Newton's 2nd Law $F = ma$ and applying it to the electrode section:

$$V - (V + dV) = \rho A dx \frac{\partial^2 w}{\partial t^2}$$

$$\therefore \rho A dx \frac{\partial^2 w}{\partial t^2} = -dV \tag{1}$$

where ρ is the wing electrode density and A is wing electrode cross-sectional area. Making the Euler-Bernoulli beam theory assumption that the second derivative of electrode section angle with respect to time is negligible, $\frac{\partial^2 \theta}{\partial t^2} \approx 0$, it is assumed that the overall moment on the wing electrode section is equal to zero. Taking clockwise-positive moments about point O (Fig. S5B):

$$M + (V + dV)dx - (M + dM) = 0$$

$$\therefore (V + dV)dx - dM = 0 \tag{2}$$

To simplify these equations, say:

$$dV = \frac{\partial V}{\partial x} dx \tag{3}$$

and:

$$dM = \frac{\partial M}{\partial x} dx \tag{4}$$

Substituting (3) into (1):

$$\rho A \frac{\partial^2 w}{\partial t^2} = -\frac{\partial V}{\partial x} \tag{5}$$

Substituting (3) and (4) into (2):

$$V dx + \frac{\partial V}{\partial x} dx^2 - \frac{\partial M}{\partial x} dx = 0$$

dx is small, $\therefore dx^2 \approx 0$, so:

$$V = \frac{\partial M}{\partial x} \tag{6}$$

Substituting (6) into (5):

$$\rho A \frac{\partial^2 w}{\partial t^2} = -\frac{\partial^2 M}{\partial x^2} \tag{7}$$

Taking the Euler-Bernoulli beam theory assumption that:

$$M = EI \frac{\partial^2 w}{\partial x^2} \tag{8}$$

where E is the Young's Modulus of the wing electrode, and I is its second moment of area in the direction of bending. Substituting (8) into (7):

$$\rho A \frac{\partial^2 w}{\partial t^2} = -\frac{\partial^2}{\partial x^2}\left(EI \frac{\partial^2 w}{\partial x^2}\right)$$

Making a uniform beam assumption, i.e. ρ, A, E and I are constant, leads to:

$$\rho A \frac{\partial^2 w}{\partial t^2} = -EI \frac{\partial^4 w}{\partial x^4}$$

$$\therefore \frac{\partial^2 w}{\partial t^2} + \frac{EI}{\rho A} \frac{\partial^4 w}{\partial x^4}$$

This can be solved using separation of variables. Assume that $w(x,t) = W_x(x)W_t(t)$, i.e. the deflection of the electrode at a given position x and time t can be described by multiplying together two independent functions: W_x which varies only with x and W_t which only varies with t. This assumption leads to:

$$\frac{\partial^2 W_t}{\partial t^2} W_x + \frac{EI}{\rho A} \frac{\partial^4 W_x}{\partial x^4} W_t$$

$$\therefore -\frac{\partial^2 W_t}{\partial t^2} \frac{1}{W_t} = \frac{EI}{\rho A} \frac{\partial^4 W_x}{\partial x^4} \frac{1}{W_x} \tag{9}$$

Since each side of (9) only varies with t or x respectively, both sides must be constant. Considering the left side of (9):

$$-\frac{\partial^2 W_t}{\partial t^2} \frac{1}{W_t} = C$$

$$\therefore \frac{\partial^2 W_t}{\partial t^2} + CW_t = 0$$

This is the equation for simple harmonic motion, which has the solution $W_t = B\cos(\omega t + \varphi)$ where B is amplitude, ω is resonant frequency and φ is phase. This implies $C = \omega^2$, therefore:

$$\frac{\partial^2 W_t}{\partial t^2} + \omega^2 W_t = 0 \quad (10)$$

Substituting (10) into (9):

$$\omega^2 = \frac{EI}{\rho A}\frac{\partial^4 W_x}{\partial x^4}\frac{1}{W_x}$$

$$\therefore \frac{\partial^4 W_x}{\partial x^4} - \beta^4 W_x = 0$$

where

$$\beta^4 = \frac{\rho A \omega^2}{EI}$$

This can be solved using the solution:

$$W_x = C_1 \cosh \beta x + C_2 \sinh \beta x + C_3 \cos \beta x + C_4 \sin \beta x \quad (11)$$

To find the values of C_1, C_2, C_3 and C_4, the boundary conditions for the electrode must be considered. The wing electrode is assumed to be a cantilever beam, built-in at position $x = 0$ and free at position $x = L$. As such, the following four boundary conditions apply:

$$W_x(0) = 0 \quad (12)$$

$$\frac{\partial W_x(0)}{\partial x} = 0 \quad (13)$$

$$M(L) = 0 \quad (14)$$

$$V(L) = 0 \quad (15)$$

Combining (8) and (14):

$$M(L) = EI\frac{\partial^2 W_x(L)}{\partial x^2} W_t = 0$$

$$\therefore \frac{\partial^2 W_x(L)}{\partial x^2} = 0 \quad (16)$$

Combining (6), (8) and (15):

$$V(L) = \frac{\partial}{\partial x} EI \frac{\partial^2 W_x(L)}{\partial x^2} W_t = 0$$

$$\frac{\partial^3 W_x(L)}{\partial x^3} = 0 \quad (17)$$

The first, second and third derivatives of (11) are required:

$$\frac{\partial W_x}{\partial x} = \beta(C_1 \sinh \beta x + C_2 \cosh \beta x - C_3 \sin \beta x + C_4 \cos \beta x) \tag{18}$$

$$\frac{\partial^2 W_x}{\partial x^2} = \beta^2(C_1 \cosh \beta x + C_2 \sinh \beta x - C_3 \cos \beta x - C_4 \sin \beta x) \tag{19}$$

$$\frac{\partial^3 W_x}{\partial x^3} = \beta^3(C_1 \sinh \beta x + C_2 \cosh \beta x + C_3 \sin \beta x - C_4 \cos \beta x) \tag{20}$$

Combining (11) and (12):

$$C_1 + C_3 = 0$$

$$\therefore C_3 = -C_1 \tag{21}$$

Combining (13) and (18):

$$C_2 + C_4 = 0$$

$$\therefore C_4 = -C_2 \tag{22}$$

Combining (16), (19), (21) and (22):

$$C_1 \cosh \beta L + C_2 \sinh \beta L + C_1 \cos \beta L + C_2 \sin \beta L = 0$$

$$\therefore C_1(\cosh \beta L + \cos \beta L) + C_2(\sinh \beta L + \sin \beta L) = 0 \tag{23}$$

Combining (17), (20), (21) and (22):

$$C_1 \sinh \beta L + C_2 \cosh \beta L - C_1 \sin \beta L + C_2 \cos \beta L = 0$$

$$\therefore C_1(\sinh \beta L - \sin \beta L) + C_2(\cosh \beta L + \cos \beta L) \tag{24}$$

Rearranging (23):

$$C_2 = -C_1 \frac{\cosh \beta L + \cos \beta L}{\sinh \beta L + \sin \beta L} \tag{25}$$

Substituting (25) into (24):

$$C_1(\sinh \beta L - \sin \beta L) - C_1 \frac{(\cosh \beta L + \cos \beta L)^2}{(\sinh \beta L + \sin \beta L)} = 0$$

$$\therefore (\sinh \beta L + \sin \beta L)(\sinh \beta L - \sin \beta L) - (\cosh \beta L + \cos \beta L)^2 = 0$$

$$\therefore \sinh^2 \beta L - \sin^2 \beta L - \cosh^2 \beta L - 2 \cosh \beta L \cos \beta L - \cos^2 \beta L = 0$$

$$\therefore 2\cosh\beta L\cos\beta L + \sin^2\beta L + \cos^2\beta L + \cosh^2\beta L - \sinh^2\beta L = 0$$

This can be solved using the trigonometric and hyperbolic identities, $\sin^2 x + \cos^2 x = 1$ and $\cosh^2 x - \sinh^2 x = 1$:

$$\therefore 2\cosh\beta L\cos\beta L + 1 + 1 = 0$$

$$\therefore \cosh\beta L\cos\beta L = -1 \qquad (26)$$

(26) must be solved numerically, and has infinite solutions:

$$\beta_1 \approx \frac{0.5969\pi}{L}$$

$$\beta_2 \approx \frac{1.495\pi}{L}$$

$$\beta_3 \approx \frac{2.500\pi}{L}$$

...

Each solution represents a normal mode of vibration of the wing electrode at a resonant frequency. The general motion of the wing electrode is a superposition of normal modes to infinity.

Combining (11), (21), (22) and (25):

$$W_x = C_1\cosh\beta x - C_1\frac{\cosh\beta L + \cos\beta L}{\sinh\beta L + \sin\beta L}\sinh\beta x - C_1\cos\beta x + C_1\frac{\cosh\beta L + \cos\beta L}{\sinh\beta L + \sin\beta L}\sin\beta x$$

$$\therefore W_x = C_1\left(\cosh\beta x - \cos\beta x - \frac{\cosh\beta L + \cos\beta L}{\sinh\beta L + \sin\beta L}(\sinh\beta x - \sin\beta x)\right)$$

Recall that $w(x,t) = W_x(x)W_t(t)$ and $W_t = B\cos(\omega t + \varphi)$. B represents the amplitude of flapping. As such, we want to choose C_1 such that $W_x(L) = 1$ and B represents the maximum amplitude of the wing electrode tip (i.e., W_x varies between 0 and 1, and is multiplied by B, which is the maximum amplitude of flapping). Numerically evaluating $W_x(L)$ with $\beta = \beta_1$ results in $W_x(L) = 2C_1$, therefore C_1 is chosen as $\frac{1}{2}$:

$$\therefore W_x = \frac{1}{2}\left(\cosh \beta x - \cos \beta x - \frac{\cosh \beta L + \cos \beta L}{\sinh \beta L + \sin \beta L}(\sinh \beta x - \sin \beta x)\right) \tag{27}$$

These are the mode shapes of the wing electrode. Recall again that $w(x,t) = W_x(x)W_t(t)$ and $W_t = B\cos(\omega t + \varphi)$. As mentioned, the general solution for the equation of motion of the wing electrode is the superposition of all normal modes to infinity:

$$w(x,t) = \sum_{n=1}^{\infty} \frac{1}{2} B_n \cos(\omega_n t + \varphi_n)\left(\cosh \beta_n x - \cos \beta_n x - \frac{\cosh \beta_n L + \cos \beta_n L}{\sinh \beta_n L + \sin \beta_n L}(\sinh \beta_n x - \sin \beta_n x)\right) \tag{28}$$

where each value of β_n may be found numerically using (26). Each resonant frequency can also be found, recalling that $\beta^4 = \frac{\rho A \omega^2}{EI}$:

$$\therefore \omega_n = {\beta_n}^2 \sqrt{\frac{EI}{\rho A}} \tag{29}$$

In the case of the Liquid-amplified Zipping Actuator (LAZA), flapping occurs almost entirely in the first mode. Furthermore, we choose $t = 0$ to occur at maximum displacement (the wing electrode is fully deflected, and its speed is zero), such that $\varphi = 0$. The equation of motion of the wing electrode thus becomes:

$$w(x,t) \approx \frac{1}{2} B_1 \cos(\omega_1 t)\left(\cosh \beta_1 x - \cos \beta_1 x - C_{mode}(\sinh \beta_1 x - \sin \beta_1 x)\right) \tag{30}$$

where

$$C_{mode} = \frac{\cosh \beta_1 L + \cos \beta_1 L}{\sinh \beta_1 L + \sin \beta_1 L}$$

and β_1 is the first solution to $\cosh \beta L \cos \beta L = -1$, $\beta_1 \approx \frac{0.5969\pi}{L}$.

The flapping angle can be calculated using the slope of the wing electrode, $\frac{\partial w}{\partial x}$:

$$\frac{\partial w}{\partial x}(x,t) = \frac{1}{2}\beta_1 B_1 \cos(\omega_1 t)\left(\sinh \beta_1 x + \sin \beta_1 x - C_{mode}(\cosh \beta_1 x - \cos \beta_1 x)\right) \tag{31}$$

Flapping angle, $\theta(t)$, the angle of the wing electrode at its tip ($x = L$), may then be calculated using:

$$\theta(t) = \tan^{-1}\frac{\partial w}{\partial x}(L,t) \quad (32)$$

The kinetic energy of the wing electrode, E_k, may be calculated using:

$$E_k = \int_0^L \frac{1}{2}\mu\left(\frac{\partial w}{\partial t}\right)^2 dx$$

where μ is mass per unit length, i.e. $\mu = \rho A$:

$$\therefore E_k = \frac{1}{2}\rho A\int_0^L \left(\frac{\partial w}{\partial t}\right)^2 dx \quad (33)$$

$\frac{\partial w}{\partial t}$ may be calculated by differentiating (30) with respect to time:

$$\frac{\partial w}{\partial t}(x,t) = -\frac{1}{2}B_1\omega_1\sin(\omega_1 t)\big(\cosh\beta_1 x - \cos\beta_1 x - C_{mode}(\sinh\beta_1 x - \sin\beta_1 x)\big) \quad (34)$$

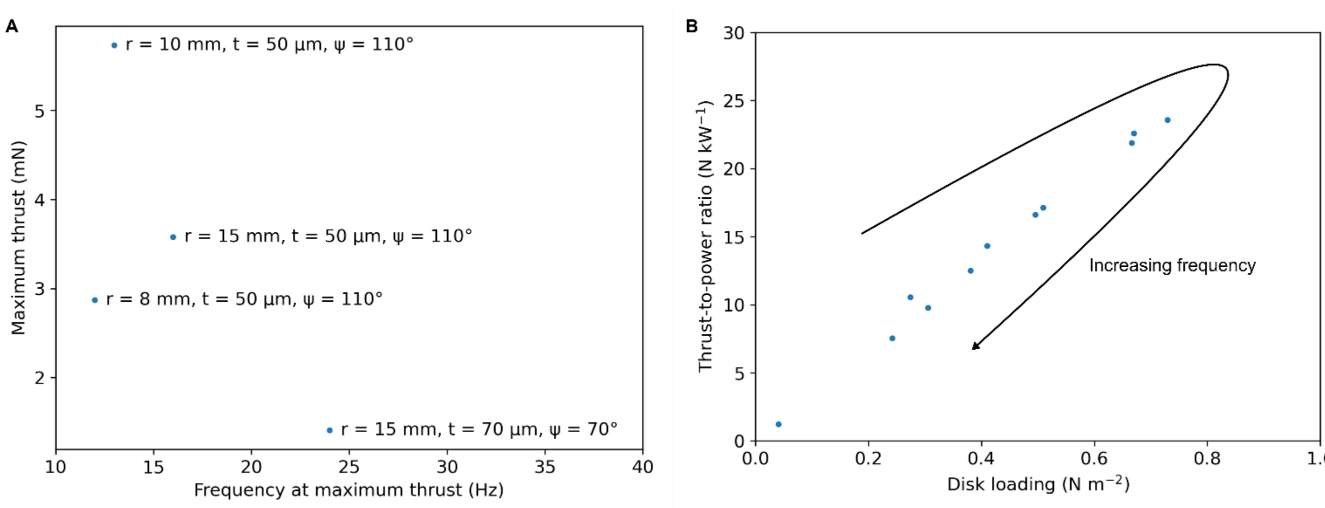

Fig. S1. Maximum thrust and thrust-to-power ratio for passively pitching wing Liquid-amplified Zipping Actuators systems. (**A**) Maximum thrust generated for a subset of tested systems. Points are labelled with the radius of curvature of the chassis electrodes, r, wing electrode thickness, t, and the maximum swept pitching angle of the wing, ψ. All wings had a wing length, $l = 50$ mm and wing chord length, $c = 20$ mm. (**B**) Thrust-to-power ratio plotted against disk loading for the highest thrust system. As frequency increases, thrust first increases as the system approaches resonance, and then decreases as frequency is further increased. This variation in thrust first increases and then reduces both thrust-to-power ratio and disk loading, resulting in the observed positive correlation. Future systems that achieve hovering flight will be subject to further investigations into the relationship between thrust-to-power ratio and disk loading.

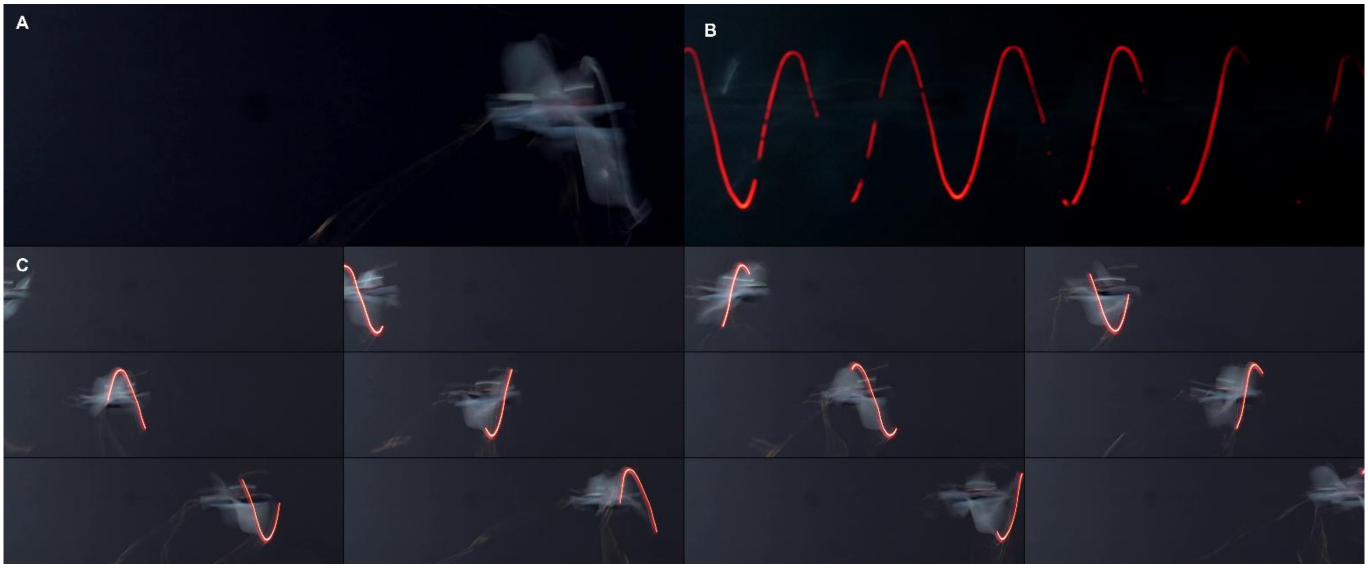

Fig. S2. Path of a horizontally moving LAZA system's wing tip. (**A**) Image from video of a horizontally moving LAZA system filmed at 25 frames per second (FPS). (**B**) Long exposure (1 second) photograph of a horizontally moving LAZA system with a red LED mounted on its wing tip. (**A**) and (**B**) were combined to Produce Fig. 6C. (**C**) 12 frames taken from a 25 FPS video of a horizontally moving LAZA system with a red LED mounted on its wing tip.

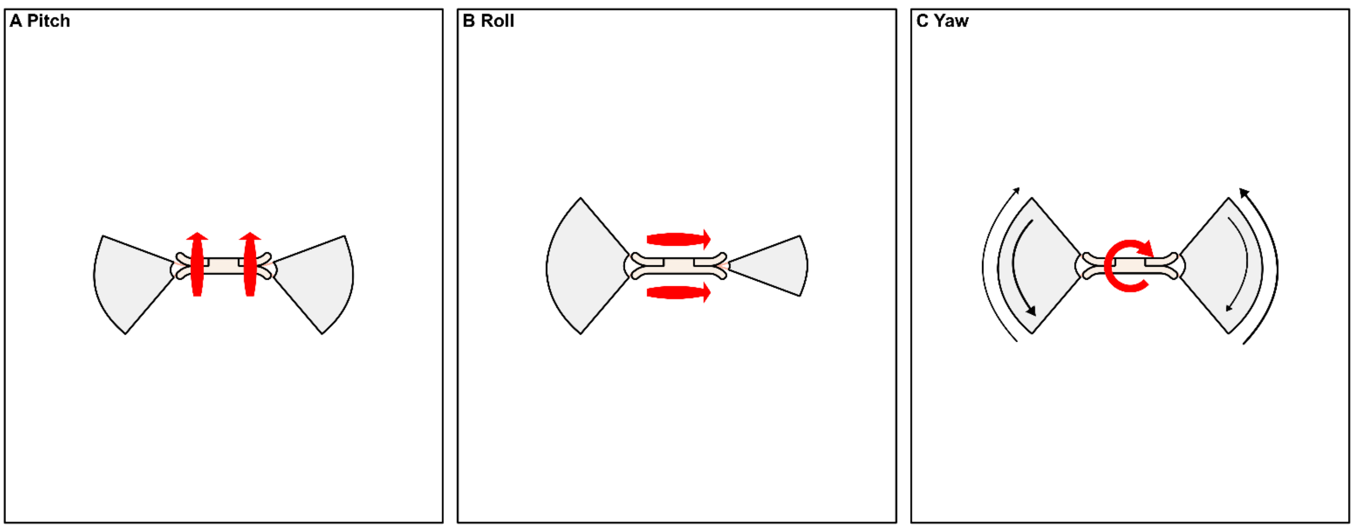

Fig. S3. Attitude control strategies for flapping MAVs. (**A**) Pitch control can be achieved by altering the relative amplitude of upstroke compared with downstroke. (**B**) Roll control is achieved by controlling the relative amplitude of opposing wings. (**C**) Yaw control requires modulation of the velocity of upstroke compared with downstroke.

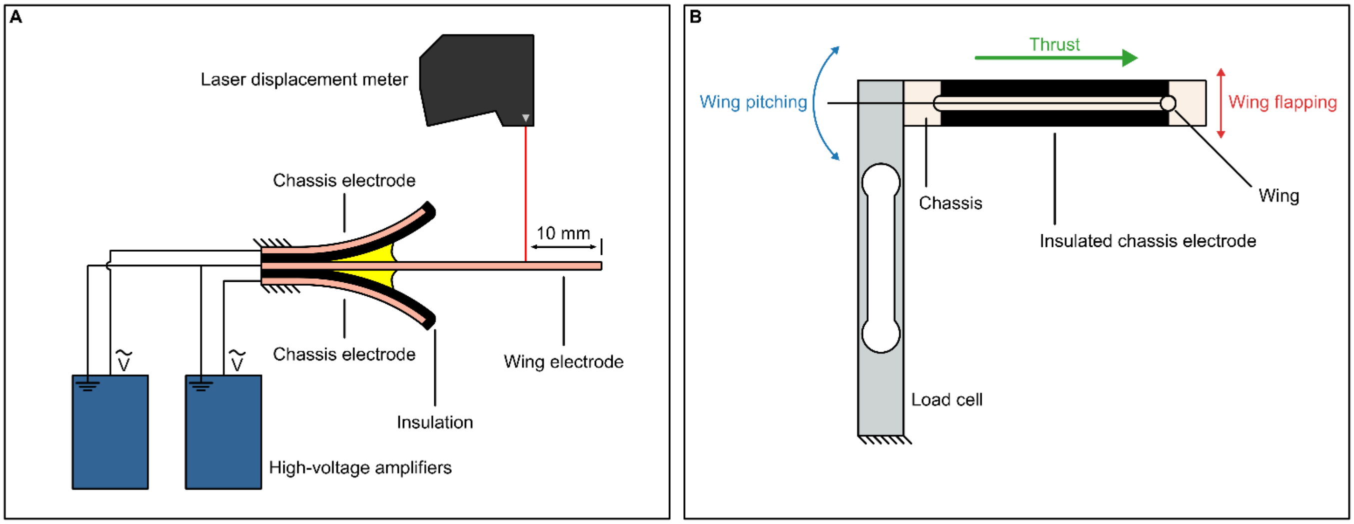

Fig. S4. Experimental setup for LAZA characterization. (**A**) Displacement characterization. High voltage was provided by two high-voltage amplifiers (10HVA24-BP1, UltraVolt, USA), and the movement of the wing electrode was recorded using a laser displacement meter ((LK-G402, Keyence, Japan). The laser beam was pointed directly downwards and was targeted 10 mm from the end of the flapping beam such that displacement could be reliably recorded even during flapping (whereby the horizontal position of the wing tip moves sideways as the wing moves up and down). (**B**) Thrust characterization. High voltage is provided by high-voltage amplifiers (not drawn) as in (**A**), and the flapping MAV is mounted to a load cell (TAL221, HT Sensor Technology Co., Ltd., China) to record thrust.

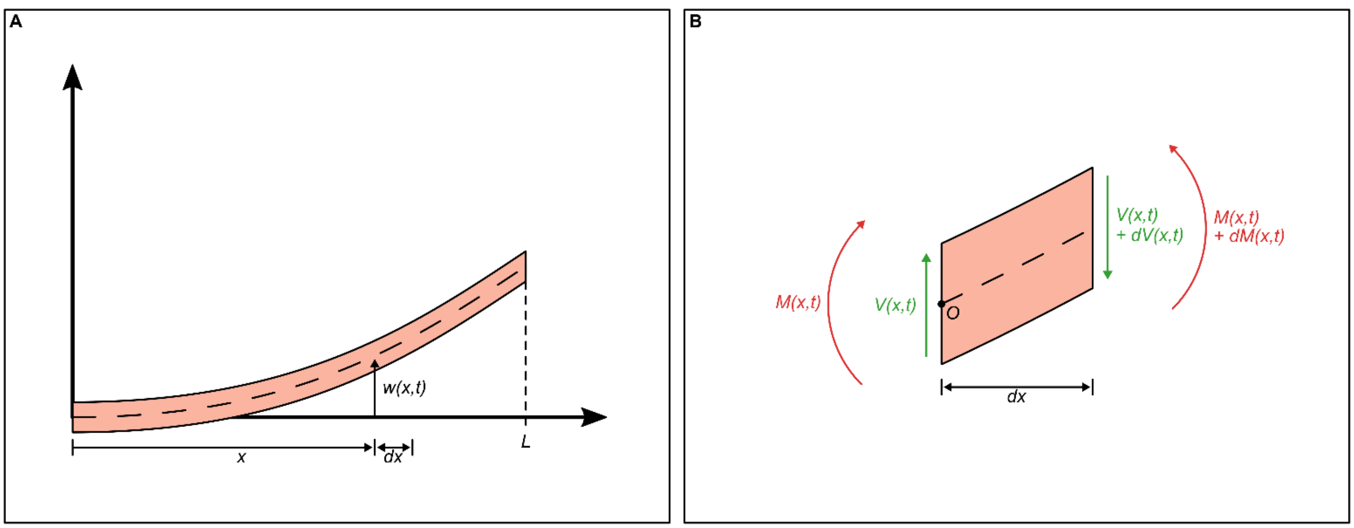

Fig S5. Wing electrode modelling. (**A**) Diagram of wing electrode of length L in bending. At position x and time t, the displacement from the rest position is $w(x,t)$. (**B**) A section of the wing electrode of length dx at position x. The moments (red) and shear forces (green) acting on the section are shown. Also shown is a chosen point O, about which moments are taken.